# High-Speed Nanorobot Position Control Inside A Scanning Electron Microscope

**Daniel Jasper**[1], **Claas Diederichs**[2],
**Christoph Edeler**[3], and **Sergej Fatikow**[4], Non-members

## ABSTRACT

Closed-loop nanorobot control performance is a key challenge on the way to high-throughput nanohandling. Currently, the limited update rate, long latency and unpredictable jitter of tracking based on scanning electron microscope images are a major bottleneck for such closed-loop control. A new approach for high-speed position sensing relying on line scans of a scanning electron microscope is adapted into the control loop of a mobile nanorobot. Several evaluation measurements show the system's unprecedented performance in terms of speed, resolution and accuracy. In only 60 ms, the employed mobile nanorobot can be positioned with a precision of 20nm in multiple degrees of freedom.

**Keywords**: Electron microscope, Nanorobot, Control

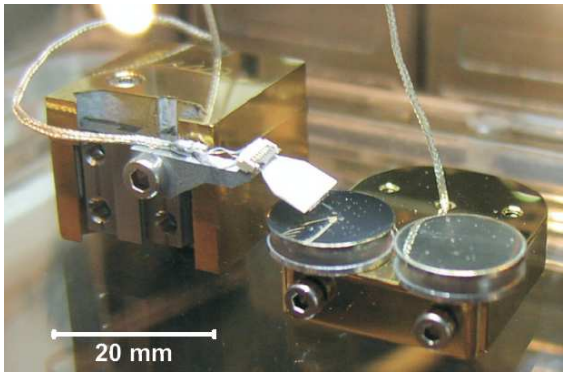


***Fig.1:*** *Nanorobotic handling cell consisting of two mobile robots. Left: tool robot carrying a microgripper, right: stage robot with two sample stubs.*

## 1. INTRODUCTION

Nanoobjects such as carbon nanotubes (CNTs) and other nanowires have become of significant interest for both the research community and industrial applications. In order to characterize these structures and in order to build nanocomponent-based devices, nanorobotic systems have been successfully applied [14]. For simplicity, such systems are called nanohandling robots or nanorobots throughout this paper as they can move and manipulate objects with nanometric precision. The size of the nanorobots themselves however is a few $cm^3$. Sensory feedback is a major challenge on the way to high throughput industrial application, as the exact relative position of tools and nanoobjects is hard to measure. Practically, the scanning electron microscope (SEM) is the only device that can be used to derive the required feedback. Optical microscopes have insufficient resolution. Atomic force microscopes as well as transmission electron microscopes have sufficient resolution, but they have a limited working range making the coarse approach tedious. Furthermore, they provide limited space to integrate nanorobotic systems. It is infeasible to control the relative position between a tool and an object only using sensors that are local to a single nanopositioner. Even with significant calibration effort, such sensors cannot be used for relative positioning because of multiple adverse effects on the nanoscale, e.g. drift.

Using the SEM as feedback for nanohandling has been applied successfully in a variety of different handling setups [5, 6]. Recently, mobile nanorobots have become a versatile and reliable tool in such setups [7] and are thus used as the basis for this paper. Section 2 investigates some key characteristics of these robots with respect to closed-loop control performance. In particular, it is shown that the available force and thus the acceleration are not limiting factors for closed-loop nanopositioning. In combination with sophisticated image processing algorithms, the SEM can be used to obtain positions [8], forces [9], quality control [10], etc. For closed-loop control, however, the combination of SEM-imaging and image processing is inefficient due to several downsides described in Section 3. Section 4 then describes a new approach to position measurements which is then integrated into a closed-loop control algorithm in Section 5. A detailed evaluation of both sensor and closed-loop control system is done in Section 6. Section 7 contains conclusions and an outlook on future works.

Manuscript received on July 28, 2010 ; revised on , .
This paper is extended from the paper presented in ECTI-CON 2010.
[1,2,3,4] The authors are with Division of Microrobotics and Control Engineering University of Oldenburg Oldenburg, Germany, E-mail: daniel.jasper@uni-oldenburg.de, Claas.Diederichs@Informatik.Uni-Oldenburg.DE,christoph.edeler@uni-oldenburg.de and fatikow@uni-oldenburg.de

## 2. NANOROBOTS

A basic nanohandling robot cell can be composed using two mobile robots - a tool robot and a stage robot (see Fig. 1). The mobile nanohandling robots used in this paper have been extensively described in several publications [7], [11], [12]. Mobile robots have several advantages over Cartesian systems with multiple linear positioners. They offer multiple degrees of freedom (DoF, seven in this robot cell) and can be employed under minimal space and infrastructure requirements. The two robots in Fig. 1 can operate on any at surface and occupy only a few cm3. Furthermore, in comparison to Cartesian systems, they other a short and direct force ow, because of the compact design and the multi-DoF in-plane actuator. This reduces vibrations and drift effects. The stick-slip actuation described below provides a high positioning resolution and smooth, almost vibration-free motion. This is in contrast to other existing nanohandling robot systems. Three of such systems are brie y described to outline the performance of our approach: The Nanowalker, the robot based on the Micron project and the Arripede robot. The Nanowalker is a robot with dimensions of approximately 1 cubic inch using three piezotubes as legs [13, 14]. Each tube can be actuated using four electrodes. Thus, motions in three DoF of each foot are possible. This allows for several types of Stick-Slip motion. One type of motion can be the actuation of just a single foot followed by the other feet. This results in comparatively slow motion with good repeatability. Another type of motion is to actuate all legs at the same time. This results in high velocities. However, repeatability decreases. Generally, working conditions are critical. Minor changes e.g. in the robot's weight or the foot geometry can result in unpredictable results. For this reason the system is not robust enough for reliable operation in a closed loop control. The robot based on the Micron project is based on actuation of piezoelectric plates to shift hemispheres, which are in contact with the working surface [1517]. The dimensions are in the range of 1 cubic inch. A large benefit compared to the Nanowalker is that it can be fabricated more easily. In combination with a rotatory lifting axis, the system exhibits four DoF. Velocities up to several mms can be achieved. A large drawback is the operation directly on the working surface, which causes wear and can make many operations performed in the same place dificult. A completely different approach is the Arripede robot [18, 19]. It is built using very fragile structures etched from silicon. The dimensions are in the range of single cubic millimeters with a weight of several grams. The motion principle is similar to the Stick-Slip principle (crawling motion). Six legs are in contact with the working surface. The legs are actuated electrothermally one after another. A steering motion to the sides could be achived yet. Thus, two DoF are realized. The approach is interesting in terms of miniaturization. However, high-speed closed loop control is still a challenge.

### 2.1 Stick-slip actuation

The actuators are based on the stick-slip principle. Stick-slip steps are generated by a sawtooth-shaped control signal, where a stick-phase is followed by a short slip-phase [7]. Practically, a stick-slip-step starts at zero voltage and the actuator is slowly de ected (piezoactuator with ruby hemispheres in Fig 2b and 2c). When reaching the full amplitude, the inverse voltage is applied rapidly and the slip is performed. The ruby hemispheres will slip over the steel sphere which is held in place by inertia. Finally, the control voltage decreases to zero and the second half of the stick-phase is executed. This procedure has the advantages that the voltages are zero after each step and that the actuator conditions before each step are virtually equal.

With the sketched stick-slip principle and piezoactuators made of PZT-5H, the step size of the device can be 130nm with 300 Vpp, or smaller. In combination with control frequencies up to 40 kHz and more, velocities of 6 mm/s can be reached. Although the repeatability of e.g. the step size is in the range of less than 2%, friction conditions have a great in uence on the stick-slip characteristics. Generally, these conditions include:

- Materials of the friction pair,
- surface roughness, lubrication, hardness, etc.,
- normal force in the friction contact,
- dependency on the lateral velocity (Stribeck),
- dwell times and
- wear.

Due to the fact that ruby hemispheres and hardened spheres from ball bearings are used, wear is negligible. This is the main motivation for the robot's design [11]. Notice that most of the mentioned effects are of nonlinear character. For understanding the stick-slip drive, two types of friction contacts have to be analyzed to be sure that the model of Fig. 2 is correct:

- steel sphere $\leftrightarrow$ working surface and
- ruby hemispheres $\leftrightarrow$ steel sphere.

Unfortunately, the exact characteristics of these contacts are unknown [12]. Measurements are hard to accomplish due to the high dynamics and the required time and position resolutions. Furthermore, many different parameters additional to friction in uence the drive's function: signal amplitude and frequency, mass and inertia of the steel spheres and the robot, attraction forces of the permanent magnets holding the steel spheres in position, rigidity of the actuators and vibrations.

According to [12], there is most likely no sliding between steel sphere and working surface. Experiments in which the robot moves widely independent of the type of the working surface further indicate

that the drive is mostly independent of this friction coefficient.

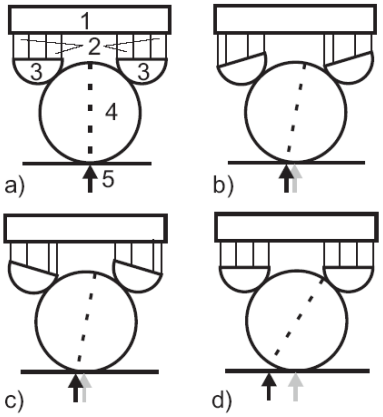


***Fig.2:*** *Sketch of the stick-slip actuation of the mobile nanohandling robots. 1: robot platform, 2: piezoactuators, 3: ruby hemispheres, 4: steel sphere, 5: working surface with arrow marker. From a) to b), the first half of the stick is performed. From b) to c), the slip happens. Although the ruby hemispheres change their position, the robot remains in position. The final stick transition is shown from c) to d) completing the step.*

This can be explained by two considerations. Firstly, the friction coefficient $\mu$ between the ruby hemispheres and the steel spheres is in the range of 0:1. This is assumed due to similar friction pairs with hard and at surfaces. The friction coefficient on any practical working surface is higher, e.g. approx. 0:5 on glass. Secondly, the inertia of the steel sphere works against the friction contact between ruby hemispheres and steel sphere but not against the friction contact between steel sphere and working surface. Thus, the friction contact between the ruby hemispheres and the steel sphere limits the robot's force.

### 2.2 Robot dynamics: Theory and measurement

Results of extensive tests have shown that the amplitude of the control signal and the normal force determine the force which can be generated by a microstickslip drive. For investigations in this paper, only the force at full control amplitude is of interest to calculate acceleration performance. Thus, the normal force is the most important parameter

From theory, the static robot's force $F_{robot}$ is

$$F_{robot} = \mu_{static} \cdot F_{normal} = \mu \cdot m_{robot} \cdot g. \quad (1)$$

With the robot's mass of 0.03 kg, Frobot can be calculated to be approximately 300 mN. The magnet's force can be neglected in this calculation, because it

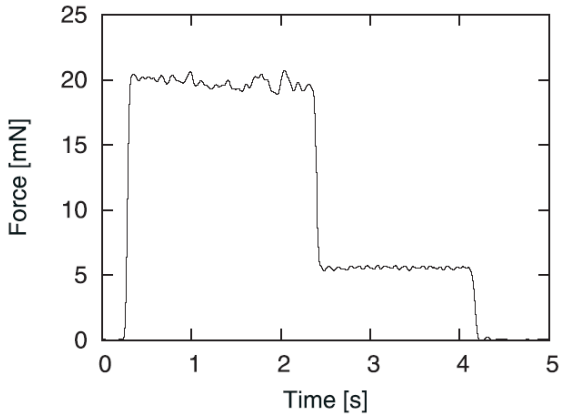


***Fig.3:*** *Measurement of the force the mobile robot can exert on an obstacle (load cell). From 0.15 s to 2.2 s, the sawtooth-signal is applied and a force of 20mN is generated. At 2.2 s, the control signal is switched off. A force of 5.5mN remains due to the elasticity of the load cell. At 4.1 s, the robot is moved into the opposite direction and the force decreases to zero.*

is in the range of only 10 mN. The friction coefficient is estimated to 0.1. Thus, the upper bound on the generated force should be 30 mN. Due to the dynamic behavior of the stick-slip drive, the real force is assumed to be on the same order but lower, e.g. 50%. However, this calculation involves, that all friction contacts of the robot - each with a low normal force - can be modelled as a single friction contact with full normal load. Other in uences such as the cable are neglected. Thus, the final theoretic value for the generated force is 15 mN. To validate the theoretic derivation, a measurement of the blocking force of the robot was performed. A horizontally mounted miniature load cell (Honeywell, model 11) was used to measure the force. Fig 3 shows the result. While the control signal is applied, the measured force uctuates between 18 and 21 mN. With control switched off, a "static" force remains, likely caused by the compliance of the load cell. Finally, the force decreases to zero when the robot is retracted. It can be concluded that the mobile nanohandling robots can create forces in the range of 20 mN. As will be seen in Section 5, the generated accelerations are currently sufficient for high performance manipulation operations. The robot can almost instantly reach any required velocity.

## 3. KEY CHALLENGE: SENSOR PERFORMANCE

Over the past years, a variety of different object recognition and object tracking algorithms have been adapted for SEM image processing and thus tracking of nanohandling robots. Widely applied are variants of cross correlation and active contours (also known

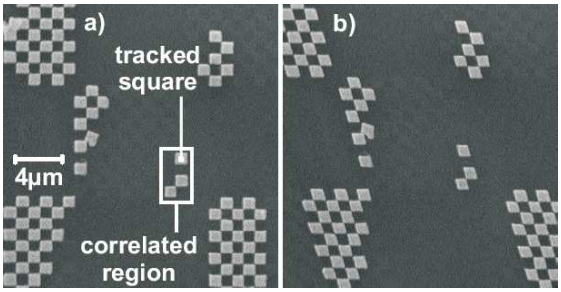


***Fig.4:*** *Chessy SEM-calibration pattern: a) stationary and b) moving right at a constant 100 µm/s.*

as snakes) [9]. While these algorithms have different advantages and disadvantages, their performance with respect to the above-mentioned characteristics are comparable, because they all work on images and are executed on a computer. Thus, in this paper, a normalized cross correlation algorithm is used as comparison. Other image-based algorithms can have slightly different characteristics, but as the SEM image acquisition itself is the major bottleneck there is no vastly superior algorithm. This is further assured by choosing almost ideal image acquisition parameters. A high specimen current (also known as spot size) leads to a high signal-to-noise ratio despite the 25 Hz frame rate on a 512×256 pixel sized region of interest (RoI). The pattern used for correlation can be seen in Fig. 4a, has a high contrast and is significantly different from other objects. Image processing was performed on a quad-core computer with no other significant CPU load.

For cross correlation, the maximum movement speed is limited by two factors. Firstly, the tracked pattern must not leave the scanned RoI. During a tracked motion, the RoI can be repositioned after each frame, but there is still a speed limit, as the pattern must not leave the RoI between two consecutive image updates. Secondly, because of the sequential line-wise scanning, the motion distorts the object as can be seen in Fig. 4b. For obvious reasons, this distortion makes recognizing an object hard and in this case lowers the correlation score. Fig. 5 shows the correlation score for different movement velocities. At movements velocities ¡10 $\mu$m/s, the correlation score remains at an almost constant value of 0.9. It does not reach 1.0 because of the noise in the SEM images which were acquired with a relatively high update rate. The score then drops linearly and falls below 0.7 at 60 $\mu$m/s. At this point, sometimes other objects in the distorted image have similar scores and the tracking becomes unreliable. When moving with 100 $\mu$m/s as seen in Fig. 4b, tracking with cross correlation becomes all but impossible. Also, it has to be kept in mind, that image acquisition parameters are chose to ideally suit the tracking and the pattern is easily recognizable. In a real scenario, the usable speeds are likely to be lower.

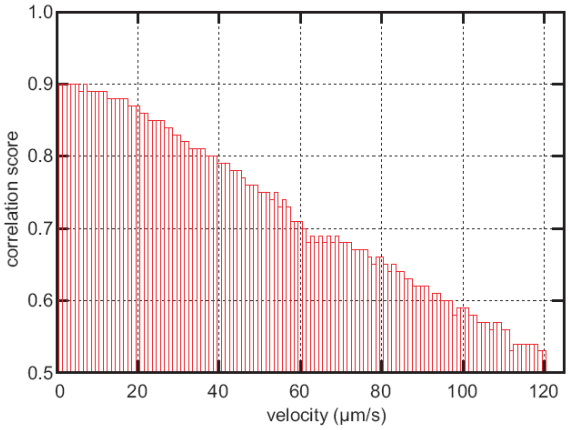


***Fig.5:*** *Correlation score at different movement velocities. At 60 µm/s, the score falls below 0.7 and tracking becomes impossible.*

Fig. 6 shows the update intervals between about 4000 samples. As expected from the 25 Hz update rate, the interval averages to 40 ms. This is a slow update rate which severely limits closed-loop control. The update rate can be increased using different approaches. Firstly, the image acquisition time could be reduced. This, however, also decreases the signal-to-noise ratio, makes object recognition more difficult and, in case of cross correlation, lowers the correlation score. Secondly, a smaller RoI could be scanned at the same pixel rate. With the approach of [20], multiple small RoIs are sufficient to determine the object's position. Small RoIs on the other hand limit the maximum movement speed, because the tracked object is more likely to leave the RoI between two sensor updates. The update rate permanently exhibits jitter in the range of ±4 ms. Around sample number 1000 and 2600, the computer seems to have executed some other processes, as the jitter suddenly rises to ±15 ms. With such a high jitter, precise PI- or PID-

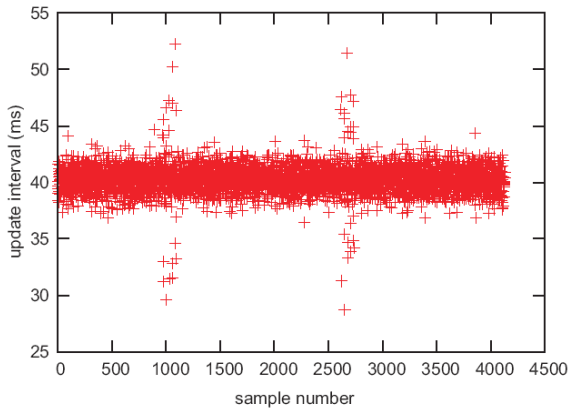


***Fig.6:*** *Sensor update interval of image-based position tracking. Around sample numbers 1000 and 2600, other tasks on the computer significantly increased the already high jitter.*

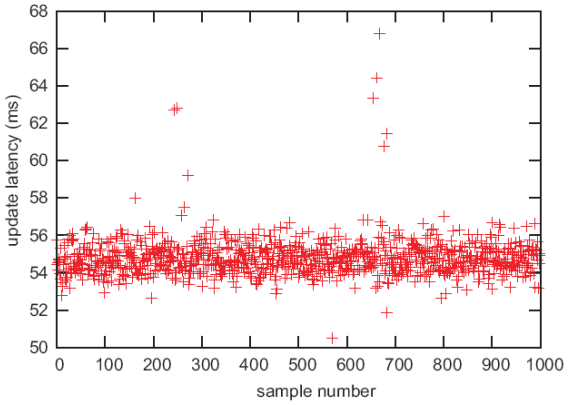


***Fig. 7:*** *Sensor update latency of image-based position tracking. The latency is composed of the time required for image acquisition, tracking calculation as well as communication overheads.*

PID-control become infeasible.

In order to characterize the update latency and corresponding jitter, the delay between a rapid movement of the robot and the corresponding sensor value change was recorded. In order to clearly attribute the jitter to the tracking algorithm, the movement was synchronized with the image updates, i.e. the robot performed a movement exactly at the end of a frame. The results are shown in Fig. 7. The average latency was approx. 55 ms, composed of 40 ms for the image acquisition and 15 ms computation time of the cross correlation. Because of the synchronous robot motion, the jitter is comparable to the update rate jitter. As four sensor updates were recorded per movement, the increased jitter around sample numbers 1000 and 2500 in Fig. 6 correspond to the increased jitter at movement numbers 250 and 625 in Fig. 7. The long 55 ms latency is problematic for closed-loop control as the controller uses obsolete data. The high jitter again makes precise PI- or PID-control infeasible.

## 4. DIRECT SEM SENSING

As pointed out above, efficient SEM-based control is not possible using image processing. Thus, a new position tracking approach was developed [21], that can determine the position of an object with high precision using only a number of line scans. In [21], a successful position tracking in x, y and rotation was shown with an update rate of up to 1 kHz and resolutions down to less than 5 nm.

For the control of the nanorobots presented in Section 2, rotational position tracking is not necessary on the small scale. If the robot moves only a few micrometers, the rotational deviation is entirely negligible. If the robot needs to be brought to the working area from another angle, the rotation itself has to be done via coarse positioning and coarse position sensing as also lateral movement of several mm or even cm is required. Thus, a simplified pattern, i.e. a single

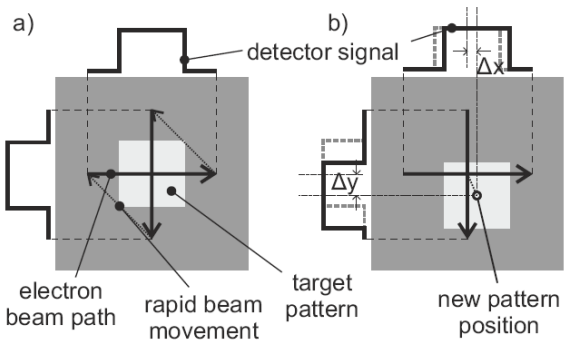


***Fig. 8:*** *Scanning pattern for point-shaped target: a) stationary and b) moving.*

point-shaped pattern, can be used (see Fig. 8). Such a pattern can easily be created using electron beam-induced deposition [22]. For this paper, a single $1\mu1$ $\mu m^2$ square of an SEM calibration grid was used (see Fig. 4). On this square-shaped pattern, a horizontal and a vertical line-scan are conducted in order to retrieve the x- and y-coordinate, respectively.

The two line scans are conducted exactly over the last known position of the square's center (see Fig. 8a). If it remains stationary, the detector shows a square wave centered around the middle of the scan. If the pattern moves, the line scans are no longer conducted over the square's center and a deviation of the detector signal during the line scan is visible (Fig. 8b).

Using a special kind of quadrature interpolation, the exact position offset $\Delta$x and $\Delta$y of the moved square can be derived from the two line scans [21]. Thus, the next line scans can be conducted over the new center and the square can be tracked continuously over long distances. Because several measurement points are recorded on each line scan (currently 512 points), the quadrature interpolation is linear even if the square does not create an exact square

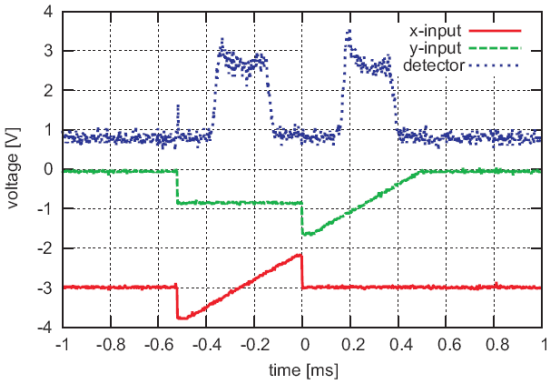


***Fig. 9:*** *Single pattern-scan taking approx. 1 ms recorded by an oscilloscope. The tracking works reliable, although the detector signal is not exactly sine-shaped.*

wave detector signal. The square-pattern used for this paper (see Fig. 4) leads to the signal shown in Fig. 9 recorded with an oscilloscope. As the linearity of the quadrature interpolation does not depend on the exact signal shape, the tracking is immune to changes in focus. Furthermore, the interpolation is immune to changes in absolute value or scale, i.e. changes in contrast and brightness [21].

The maximal movement speed that can be tracked without losing the square's position is an important property for closed-loop positioning. The position can be lost, if the square moves so far, that one of the tracked lines entirely misses it. As each scan is performed over the last known center point, this means that the square must not move more than half of its size between two position measurements. Because of a hardware limitation of the currently used scan generator, the maximum update rate of the tracking approach is approximately 500 Hz. Thus, during the 2 ms between two scans, the robot must not move more than half of the square's size, i.e. 500nm for the used 1 $\mu$m square. Thus, the theoretic limit for the trackable movement speed is 250 $\mu$m/s.

## 5. NANOROBOT CONTROL

The basic open-loop control of the mobile robots is derived in [7]. Each robot features six control channels as shown in Fig. 10a. As rotational movement is not used during nanopositioning, the robot performs purely translational movement. For this movement, three actuation amplitudes $u_1$, $u_2$ and $u_3$ are used (see Fig. 10b), enabling the robot to move into an arbitrary direction:

$$\begin{aligned} u_1 &= K \cdot p_x \\ u_2 &= -K \cdot 60 \cdot p_x + K \cdot \sin 60 \cdot p_y \\ u_3 &= -K \cdot 60 \cdot p_x - K \cdot \sin 60 \cdot p_y \end{aligned} \tag{2}$$

$K$ is a constant factor mapping the normalized desired motion components $p_x$ and $p_y$ to the maximum amplitude in Vpp. The value of $K$ is limited by the used high-voltage amplifiers and amounts to:

$$K = 300\text{Vpp} \tag{3}$$

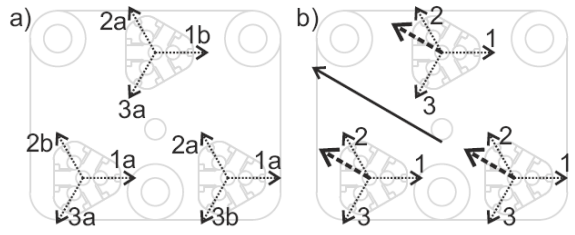


***Fig.10:*** *Control channels of a mobile nanorobot: a) All six channels, b) three channels for translational movement.*

Characterization measurements have shown that a net step length of 130nm is achieved with this amplitude [7]. It has to be noted that the total normalized length of the motion $l$ with

$$l = \sqrt{p_x^2 + p_y^2} \tag{4}$$

must not exceed 1. Otherwise, at least one of the amplitudes exceed the maximum 150 Vpp.

Based on the open-loop control and the effective tracking algorithm, a closed-loop nanorobot positioning algorithm can be implemented. There are several differences between micro-scale and macro-scaleclosed-loop control. Macro-scale control mostly solves challenges due to the dynamic behavior of systems, e.g. inertia. On the micro- and nanoscale, these effects become negligible. The mobile robot described in Section 2 has a mass $m$ of 30 g and can create a force $F$ of approximately 0.02N. Thus, its maximum acceleration a is

$$a = \frac{F}{m} = \frac{2}{3}\left[\frac{m}{s^2}\right]. \tag{5}$$

With this acceleration, the robot can reach the tracking's velocity limit $v$ of 250 $\mu$m/s within

$$t = \frac{v}{a} = 0.375[ms]. \tag{6}$$

As t is significantly below the 2 ms update rate of the sensor, acceleration effects can be neglected. The robot can be assumed to instantly change its motion behavior to any value regardless of the current state. Thus, a simple proportional controller is sufficient to perform efficient closed-loop control.

For closed-loop control, amplitude modulation is used to control the movement direction whereas frequency modulation is used to control the movement speed. The values for $p_x$ and $p_y$ are calculated from the control deviations $e_x$ and $e_y$ by calculating a normalized vector towards the target position:

$$\begin{aligned} \alpha &= \tan^{-1}(e_y/e_x) \\ p_x &= \sin\alpha \\ p_y &= \cos\alpha \end{aligned} \tag{7}$$

A simple proportional controller is then used in order to control the movement speed, i.e. the actuation frequency $f$ is calculated based on the distance to the target position and a proportional gain $K_p$:

$$f = K_p \cdot \sqrt{e_x^2 + e_y^2}. \tag{8}$$

In order to safely remain within the trackable velocity range of 250 $\mu$m/s, the step frequency is limited to 1.6 kHz which leads to a little over 200 $\mu$m/s movement speed. The closed-loop control can directly be done in the SEM's coordinate system. However, a scaling according to the SEM's magnification, i.e.

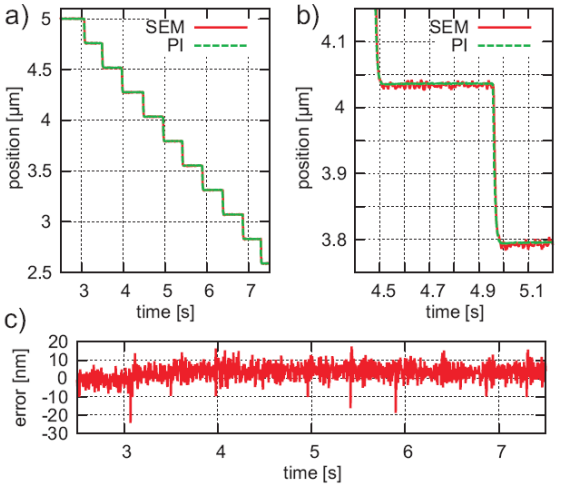


***Fig.11:*** *242nm steps performed by linear axis with capacitive readout. a) Overview, b) magnification of a single step and c) difference between the two sensors during all steps.*

view field size, should be done, so that the same gain $K_p$ can be used. $K_p$ was then chosen empirically to obtain the settling behavior described in Section 6.

## 6. EVALUATION

The first step of the evaluation was the analysis of the tracking system's performance. Several characterizations have already been conducted in [21] and are not repeated here. It was proven, that the sensor system has a high update rate and resolution while it is immune to changes in contrast, brightness and focus. Also, it was shown that the system can track with nanometric resolution over long working ranges (more than 200 $\mu$m). This evaluation thus tries to measure the system's absolute accuracy. For the measurements, the chessy calibration grid was mounted on a linear nanopositioner manufactured by Physik Instrumente (PI), Germany. The positioner uses a stacked piezoactuator and a exure hinge structure to position with nanometer resolution over a 50 $\mu$m working range. A calibrated, capacitive position sensor is used for closed-loop position control and as a reference for these measurements.

Such a sensor can offer high resolution and accuracy, but has several downsides when beeing used for closed-loop nanohandling. First, a repeated recalibration is necessary because of long-term drift, e.g. thermal drift. Second, the actual position of the nanoobject can only be precisely derived from the sensor, if the actuator's machenical joints and hinges can be assumed to be ideal. This is true for actuators based on

exure hinges, but the working range of such actuators is limited, in this case to 50 $\mu$m. Third, the SEM coordinate system itself constantly changes. The electron column becomes magnetized and charged particles within the chamber can slightly shift or distort the image. All these problems make closed-loop nanohandling difficult if only internal sensors are used.

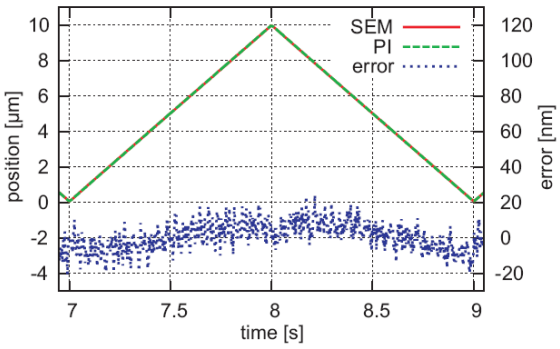


***Fig.12:*** *Linear ramp movements by axis with capacitive readout. The difference between tracking and sensor value remains below 25 nm.*

For the first measurement, the positioner was set to perform several 242 nm steps and the positions calculated using the internal sensor and the SEM-tracking were recorded simultaneously (see Fig. 11). Fig. 11a shows, that all 10 steps were tracked precisely as the two curves are virtually identical. The magnification of a single step (Fig. 11b) shows that the SEM-tracking has a slightly higher noise level but can precisely resolve the step, including the dynamic settling behavior. Fig. 11c shows the deviation between the two sensors which remains below 25 nm.

In order to fully evaluate the linearity of the position sensing, the PI positioner was then set to execute a 10 $\mu$m-long linear ramp (see Fig. 12). Again, the ramp was precisely tracked and there is no discernible difference between the two sensor outputs. The error also remains below 25 nm. The shape of the error signal suggests a minute scaling offset between the two sensors, but this offset is negligible.

After evaluating the sensor, the performance of the entire control system has to be determined. As no ref-

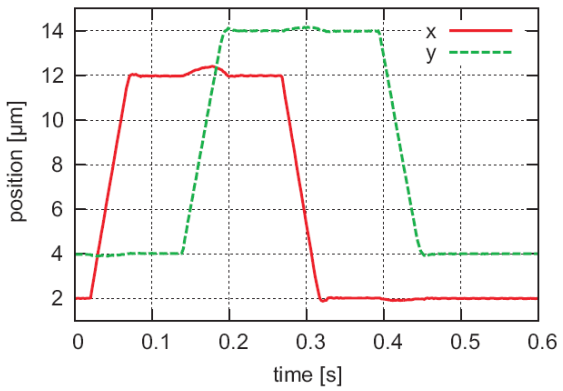


***Fig.13:*** *x- and y-coordinates while moving along a 10 $\mu$m square with closed-loop control.*

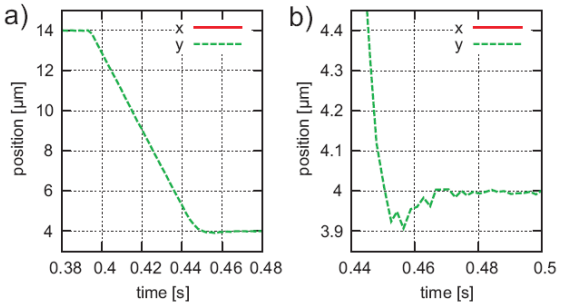


***Fig.14:*** *Ramp during a 10 µm closed-loop control step. a) Entire ramp and b) magnification of the final approach.*

erence sensor is required, the handling cell shown in Fig. 1 was used. The calibration grid was mounted onto the stage nanorobot. The robot was then moved along a 10 $\mu$m square (see Fig. 13) using closed-loop position control. The robot moves quickly and precisely to the designated target points at the corners of the square. The entire movement with 50 ms pauses at each corner was completed in less than 0.5 s. There is a small deviation from the straight line during each movement, i.e. a small x-movement during the 10 $\mu$m y-movements and vice versa. This is caused by the imperfect open-loop control, which cannot fully account for manufacturing differences and mounting conditions such as the cable position. In order to compensate for this effect, the control algorithm would need to be changed from position control to path or trajectory control.

Fig. 14 magnifies the last 10 $\mu$m control step. As expected, the robot almost instantly reaches its maximum velocity of approx. 200 $\mu$m/s which was set as a save limit for the tracking (compare Section 4). It then moves to the target position with constant velocity (see Fig. 14a) and settles to the destination quickly with a 100nm overshoot (see Fig. 14b). The entire movement is completed in approx. 60 ms. If the overshoot is problematic for a specific nanomanipulation step, it can be avoided using a smaller proportional gain $K_p$ (see Section 5) which prolongs the settling time to about 80 ms. The final accuracy with the used tracking parameters is approximately $\pm$15nm which is equal to the (tungsten cathode-based) SEM's resolution limit and should be sufficient for current nanohandling operations.

## 7. CONCLUSION AND OUTLOOK

This paper has shown that image-based position detection is a major bottleneck on the way to high-throughput nanomanipulation. Using a new position detection approach that entirely omits the process of image acquisition and image processing, a highspeed position tracking was implemented. It was shown, that the position of an object moving with up to 250 $\mu$m/s can be detected with an update rate of 500 Hz and a precision better than 15 nm. With these sensor characteristics, high-performance closedloop control could be implemented. Reaching a target point with an accuracy of 15 nm, a robot could perform controlled 10 $\mu$m steps with settling times of 60 ms. This is a major step forward and paves the way towards high-throughput nanomanipulation.

Table 1 shows a comparison of the different approaches that can be used for closed-loop positioning. Positioning based on internal sensors (IS) is the fastest, but has limited accuracy because the value due to the internal sensor's time-variant relation to the SEM's image coordinate system. Visual servoing (VS) based on SEM images is accurate but slow due to the inherent bottleneck of image acquisition. The line scan-based positioning (LS) combines a speed similar to internal sensor with the accuracy of visual servoing.

***Table 1:*** *Important tracking parameters.*

| type | $f$ | $v_{max}$ | $t_s$ | accuracy |
|---|---|---|---|---|
| IS | >1kHz | $\infty$ | 10ms | - |
| VS | <50Hz | 60 $\mu$m/s | >0.5s | + |
| LS | 1kHz | 250 $\mu$m/s | 60ms | + |

Using the work of this paper as a basis, the position control can be taken further. First, the maximum movement speed can be increased if the sensor and the controller are coupled more tightly. As the 15nm accuracy is not needed during fast movements, the controller could temporarily set the tracking algorithm to an even higher update rate. With the higher update rate, faster movements can be tracked with the downside of increased noise. For the final approach, the tracking is then changed back to a slower update rate with higher precision. Second, first tests on time-shared tracking of two objects have been conducted, i.e. two patterns are scanned sequentially. As expected, only half the update rate could be achieved, but all other characteristics remained unchanged. Third, tracking in the third dimension will be the key to a versatile application of nanohandling in SEMs. Due to their large depth of sharpness, SEMs cannot precisely determine the position of objects in the out-of-plane direction. Several image-based approaches have been implemented, e.g. deriving depth information from focus or adding a beam-deflection system for stereoscopic images. The combination of these approaches with the direct SEM-tracking is currently being analyzed.

## 8. ACKNOWLEDGMENT

Parts of this work were supported by the European Community: Project NanoHand (IP 034274).

## References


[1] J. J. Abbott, Z. Nagy, F. Beyeler, and B. J. Nelson, "Robotics in the Small, Part I: Microrobotics," *IEEE Robotics & Automation Magazine*, vol. 14, no. 2, pp. 92-103, 2007.

[2] L. Dong and B. J. Nelson, "Robotics in the Small, Part II: Nanorobotics," *IEEE Robotics & Automation Magazine*, vol. 14, no. 3, pp. 111-121, 2007.

[3] T. Fukuda, M. Nakajima, P. Liu, and H. ElShimy, "Nanofabrication, Nanoinstrumentation and Nanoassembly by Nanorobotic Manipulation," *Journal of Robotis Research*, vol. 28, no. 4, pp. 537-547, 2009.

[4] B. J. Nelson, L. X. Dong, A. Subramanian, and D. J. Bell, *Robotics Research*, ser. Springer Tractsin Advanced Robotics (STAR). Springer, 2007, vol. 28, ch. Hybrid Nanorobotic Approaches to NEMS, pp. 163-174.

[5] T. Wortmann, C. Dahmen, R. Tunnell, and S. Fatikow, "Image Processing Architecture for Real-Time Micro- and Nanohandling Applications," in *Proc. of the Eleventh IAPR Conference on Machine Vision Applications (MVA)*, Yokohama, Japan, May 2009.

[6] S. Fatikow, T. Wich, S. Kray, H. Hülsen, T. sievers, M. Jähnisch, and V. Eichhorn, "Automatic nanohandling station inside a scanning electron microscope," in *2nd Int. Conf. in Multi-Material Micro Manufacture (4M'06)*, Grenoble, France, September 2006, pp. 17-22.

[7] D. Jasper and C. Edeler, "Characterization, optimization and control of a mobile platform," in *Proc. of 6th Int. Workshop on Microfactories (IWMF)*, 2008.

[8] T. Sievers and S. Fatikow, "Real-time object tracking for the robot-based nanohandling in a scanning electron microscope," *Journal of Micromechatronics - Special Issue on Micro/Nanohandling*, vol. 3, no. 3-4, pp. 267-284(18), 2006.

[9] T. Sievers, M. Jähnisch, C. Schrader, and S. Fatikow, "Vision feedback in an automatic nanohandling station inside an SEM," in *Proc. of 6th Int. Optomechatronics Conference on Visual/Optical Based Assembly and Packaging*, SPIE's Optics East, 2006.

[10] T.Wortmann and S. Fatikow, "Carbon Nanotube Detection by Scanning Electron Microscopy," in *Proc. of the Eleventh IAPR Conference on Machine Vision Applications (MVA)*, Yokohama, Japan, May 2009.

[11] C. Edeler, "Simulation and Experimental Evaluation of Laser-Structured Actuators for a Mobile Microrobot," in *Proc. of IEEE Intl. Conference on Robotics and Automation (ICRA)*, Pasadena, CA, USA, May 2008, pp. 3118-3123.

[12] C. Edeler, D. Jasper, and S. Fatikow, "Development, Control and Evaluation of a Mobile Platform for Microrobots," in *Proc. of the 17th IFAC World Congress*, Seoul, Korea, July 2008, pp. 12739-12744.

[13] S. M. Martel, A. Saraswat, and I. W. Hunter, "Fundamentals of piezoceramic actuation for micrometer and submicrometer motions for the NanoWalker robot," *Proc. of SPIE*, vol. 4194, no. 1, pp. 82-93, 2000.

[14] S. Martel and I. Hunter, "Nanofactories based on a eet of scientific instruments configured as miniature autonomous robots," *Jornal of Micromechatronics*, vol. 2, no. 3-4, pp. 201-214, 2004.

[15] J. Brufau, M. Puig-Vidal, J. Lopez-Sanchez, J. Samitier, N. Snis, U. Simu, S. Johansson, W. Driesen, J.-M. Breguet, J. Gao, T. Velten,J. Seyfried, R. Estana, and H. Woern, "Micron: Small autonomous robot for cell manipulation applications," in *Proc. of IEEE Int. Conference on Robotics and Automation (ICRA)*, Barcelona, Spain, April 2005, pp. 844-849.

[16] W. Driesen, T. Varidel, S. Régnier, and J.-M. Breguet, "Micro manipulation by adhesion with two collaborating mobile microrobots," *Journal of Micromechanics and Microengineering*, vol. 15, pp. 259-267, 2005.

[17] J.-M. Breguet, W. Driesen, F. Kaegi, and T. Cimprich, "Applications of piezo-actuated microrobots in micro-biology and material science," in *International Conference on Mechatronics and Automation (ICMA)*, Heilongjiang, China, August 2007, pp. 57-62.

[18] R. Murthy, A. Das, and D. Popa, "ARRIpede: An Assembled Micro Crawler," in *Proc. of 8th IEEE Conference on Nanotechnology (NANO'08)*, Arlington, TX, USA, August 2008, pp. 833-836.

[19] R. Murthy and D. Popa, "A Four Degree of Freedom Microrobot with Large Work Volume," in *Proc. of IEEE Int. Conference on Robotics and Automation (ICRA)*, Kobe, Japan, May 2009, pp. 1028-1033.

[20] B. E. Kratochvil, L. Dong, and B. J. Nelson, "Real-time Rigid-body Visual Tracking in a Scanning Electron Microscope," *The International Journal of Robotics Research*, vol. 28, pp. 498-511, 2009.

[21] D. Jasper, "High-speed Position Tracking for Nanohandling inside Scanning Electron Microscopes," in *Proc. of IEEE Intl. Conference on Robotics and Automation (ICRA)*, Kobe, Japan, May 2009, pp. 508-513.

[22] T. Luttermann, T. Wich, C. Stolle, and S. Fatikow, "Development of an Automated Desktop Station for EBiD-based Nano-Assembly," in *Prof. of 2nd International Conference on Micro-Manufacturing (ICOMM)*, 2007, pp. 284-288.

**Daniel Jasper** studied Computer Science with focus on "Embedded Systems and Microrobotics" at the University of Oldenburg. In 2006 he finished his studies receiving a Diplom-Informatik degree. Since November 2006 he is working as scientific researcher at the Division Micro- robotics and Control Engineering. Within the scope of his Ph.D. thesis he is working on the control of microrobots.

**Claas Diederichs** studied computer science with focus on embedded systems and micro-robotics at the Oldenburg University. In 2007, he graduated with a diploma in computer science. After his diploma thesis at Siemens VDO (now Continental) with the title "Simulation and opti mization of two FlexRay-coupled Engine Management Systems" he worked as a developer and consultant in real-time simulation and real-time verification of commercial embedded systems. Since March 2008, he is working for the Division of Microrobotics and Control Engineering (AMiR) as a researcher with the focus on development of real-time capa- ble control of nanomanipulation systems.

**Christoph Edeler** received his degree in mechanical engineering from the Rheinisch-Westfaelische Technische Hochschule (RWTH) Aachen, Germany, with the major field "theory of design". He completed his degree with an external diploma thesis in the company CLAAS harvesting machines, Harsewinkel, Germany, finishing in March 2006. He started his research at the Division of Micro-robotics and Control Engineering (AMiR) in June 2006. His main interests are design and fabrication of piezo-driven stick-slip microactuators, simulation of stick-slip- related friction and application of such devices for position and force generating purposes.

**Sergej Fatikow** born on March 5, 1960 in Ufa, Russia, studied computer science and electrical engineering at the Ufa Aviation Technical University in Russia, where he received his doctoral degree in 1988 with work on intelligent control of complex non-linear systems. After two years of teaching in Ufa he moved to the Institute for Process Control and Robotics at the University of Karlsruhe in Germany, where he worked as a scientific researcher and since 1996 as an assistant professor. In 2000 he accepted a Professor position at the University of Kassel (Germany) and in 2001 a Full Professor position at the University of Oldenburg (Germany). Prof. Fatikow is the head of the Institute for Micro-robotics and Control Engineering. His research interests include different aspects of micro- and nanorobotics, microactuators and microsensors, intelligent control of nanohandling robot cells, and neuro-fuzzy-based robot control. He is author of two books on microsystem technology, microrobotics and microassembly, published by Springer in 1997 and by Teubner in 2000.